Osteocyte Physiology and Response to Fluid Shear Stress Are Impaired Following Exposure to Cobalt and Chromium: Implications for Bone Health Following Joint Replacement

Karan M. Shah, Peter Orton, Nick Mani, Jeremy Mark Wilkinson, Alison Gartland

Department of Oncology and Metabolism, The University of Sheffield, Beech Hill Rd, Sheffield S10 2RX, United Kingdom

Received 1 June 2016; accepted 23 September 2016
Published online 14 October 2016 in Wiley Online Library (wileyonlinelibrary.com). DOI 10.1002/jor.23449

ABSTRACT: The effects of metal ion exposure on osteocytes, the most abundant cell type in bone and responsible for coordinating bone remodeling, remain unclear. However, several studies have previously shown that exposure to cobalt (Co^{2+}) and chromium (Cr^{3+}), at concentrations equivalent to those found clinically, affect osteoblast and osteoclast survival and function. In this study, we tested the hypothesis that metal ions would similarly impair the normal physiology of osteocytes. The survival, dendritic morphology, and response to fluid shear stress of the mature osteocyte-like cell-line MLO-Y4 following exposure to clinically relevant concentrations and combinations of Co and Cr ions were measured in 2D-culture. Exposure of MLO-Y4 cells to metal ions reduced cell number, increased dendrites per cell and increased dendrite length. We found that combinations of metal ions had a greater effect than the individual ions alone, and that Co^{2+} had a predominate effect on changes to cell numbers and dendrites. Combined metal ion exposure blunted the responses of the MLO-Y4 cells to fluid shear stress, including reducing the intracellular calcium responses and modulation of genes for the osteocyte markers *Cx43* and *Gp38*, and the signaling molecules *RANKL* and *Dkk-1*. Finally, we demonstrated that in the late osteoblasts/early osteocytes cell line MLO-A5 that Co^{2+} exposure had no effect on mineralization, but Cr^{3+} treatment inhibited mineralization in a dose-dependent manner, without affecting cell viability. Taken together, these data indicate that metal exposure can directly affect osteocyte physiology, with potential implications for bone health including osseointegration of cementless components, and periprosthetic bone remodeling. © 2016 The Authors. *Journal of Orthopaedic Research* Published by Wiley Periodicals, Inc. on behalf of Orthopaedic Research Society. J Orthop Res 35:1716–1723, 2017.

Keywords: osteocytes; mechanical stimuli; bone remodeling; osseointegration; metal ions

Osteocytes account for approximately 95% of the cell population of bone, and arise as terminally differentiated osteoblasts that have become embedded in the mineralizing osteoid matrix. Osteocytes connect to other osteocytes and cells on the bone surface to form an extensive dendritic network that senses mechanical strain and renders the osteocyte as the primary mechanosensory cell within bone.[1]

The osteocyte network plays a master role in maintaining bone homeostasis through signaling pathways that orchestrate osteoblast and osteoclast activities necessary for normal bone health.[2] Osteocyte cell death and alterations in dendritic morphology and connectivity play a role in osteonecrosis of the femoral head, especially following chronic steroid treatment.[3] Decreased osteocyte dendritic connectivity is also found in osteoporosis and osteoarthritis, while osteomalacic bone exhibits an increased, but chaotic connectivity,[4,5] highlighting the importance of dendricity in pathophysiological conditions.

Successful osseointegration and survival of prosthetic joints also requires normal bone health. Data from several large national joint replacement registries have shown that hip replacement prostheses that use a large diameter metal-on-metal (MOM) bearing made of a cobalt–chromium alloy have a survivorship that is profoundly poorer than prostheses that use non-metal-on-metal bearings.[6–9] This poor survivorship is due to complications including failed prosthesis osseointegration, osteolysis, femoral neck fracture, and hypersensitivity responses, and has resulted in a requirement for the regular clinical monitoring of indwelling prostheses,[10] the recall of several prosthesis brands,[11] and litigation against their manufacturers. It has also recently become more widely recognized that wear-accelerated corrosion at taper junctions of all modular prostheses generates metallic wear debris and impairs prosthesis survival.[12–14]

Normal physiological concentrations of cobalt (Co) and chromium (Cr) in unexposed individuals are $<0.3\,\mu g/L$,[15,16] metal-on-metal bearings are known to cause an elevation in Co and Cr in both local tissues of the hip joint and systemically. In well-functioning prostheses at 10-year follow-up, median Co and Cr concentrations in the circulation have been reported to be $0.75\,\mu g/L$ (range: 0.3–$50.1\,\mu g/L$) and $0.95\,\mu g/L$ (range: 0.3–$58.6\,\mu g/L$) respectively.[17] Periprosthetic concentrations are several fold higher (median Co, $113\,\mu g/L$; median Cr, $54\,\mu g/L$),[18] while patients with failing prosthesis have reported Co and Cr concentrations as high as $528\,\mu g/L$ (range: 0–$13{,}000\,\mu g/L$) and

Karan M. Shah and Peter Orton contributed equally to this work.

J. Mark Wilkinson and Alison Gartland are the senior authors who contributed equally to this work.

Grant sponsor: ORUK; Grant number: Project 517; Grant sponsor: Arthritis Research UK; Grant sponsor: The University of Sheffield LETS SURE Scheme; Grant sponsor: Dr. Mo Sacoor MRCP Medical Elective Research Scholarship.

Correspondence to: J. Mark Wilkinson (T: +44-114-2159029; F: +44-114-2618775; E-mail: j.m.wilkinson@sheffield.ac.uk)
Correspondence to: Alison Gartland (T: +44-114-2159046; F: +44-114-2712475; E-mail: a.gartland@sheffield.ac.uk)

1,844 μg/L (range: 0–38,600 μg/L), respectively.[19] We recently demonstrated that exposure to Co^{2+} and Cr^{3+} adversely affects both osteoclast and osteoblast survival and function, including the mineralization of prosthesis surfaces in vitro, at concentrations equivalent to those found clinically.[20–22]

Previous studies have suggested that exposure to Co^{2+} in vitro has a cytotoxic and pro-inflammatory effect on osteocytes.[23–26] Here, we develop understanding in this area by examining the effects of exposure to both Co^{2+} and Cr^{3+} at clinically relevant concentrations on osteocyte physiology—in particular their survival, dendritic morphology, response to fluid shear stress (FSS), and mineralization.

MATERIALS AND METHODS

Metal Ion Preparation and Treatments

Cobalt (II) hexahydrate ($CoCl_2 \cdot 6H_2O$) and chromium (III) chloride hexahydrate ($CrCl_3 \cdot 6H_2O$) (Fluka, Gillingham, UK) served as salts for Co^{2+} and Cr^{3+}, respectively. Working concentrations of each metal ion were prepared, as previously described.[20] The stability of these metal ions in culture media has been confirmed previously using flame-atomic absorption spectroscopy.[20] Control treatment contained equivalent volume of sterile distilled water to maintain conditions, and referred to as 0 μg/L treatments.

Cell Culture

MLO-A5 cells are thought to represent the post-osteoblast, pre-osteocyte cells responsible for triggering mineralization of osteoid.[27] MLO-A5 cells were maintained at 37°C in a humidified atmosphere of 95% air and 5% CO_2 with α-MEM GlutaMAX™ (ThermoFisher Scientific, Paisley, UK) containing 100 U/ml penicillin, 100 μg/ml streptomycin, and 10% FBS (Life Technologies, Paisley, UK) (referred to as complete α-MEM).

MLO-Y4 cells were derived from the same transgenic mice as the MLO-A5 cells, but exhibit a more mature osteocyte phenotype, with characteristic dendritic morphology complemented with expression of osteocytic genes such as osteocalcin and connexin-43.[28] The cells were grown in rat-tail type 1 collagen (ThermoFisher Scientific) coated T75 flasks (0.15 mg/ml in 0.02 M acetic acid) and maintained at 37°C in a humidified atmosphere of 95% air and 5% CO_2, with α-MEM+ containing 100 U/ml penicillin, 100 μg/ml streptomycin, 2.5% FBS, and 2.5% BCS (complete α-MEM+).

MLO-Y4 Survival and Dendricity

To assess survival and dendricity, MLO-Y4 cells were cultured overnight in collagen coated 96-well plates at 2,500 cells per well in complete α-MEM+ at 37°C in a humidified atmosphere of 95% air and 5% CO_2. Subsequently, the cells were treated with vehicle (0.5% FCS supplemented α-MEM +) ± metal ion treatments for 24 h after which they were fixed and stained with 0.1% crystal violet[29] (Sigma–Aldrich, Gillingham, UK).

To quantify MLO-Y4 cell survival, cell numbers were counted from five non-overlapping random fields of view per treatment with four wells quantified for each treatment. Dendricity was assessed by counting the number of dendrites per cell and the average length of dendrites, for dendrites greater than 5 μm in length. Quantification was done using CellD imaging software (Olympus, Southend-on-Sea, UK) on 200× magnified images with Leica DMI4000B microscope.

Intracellular Calcium ($[Ca^{2+}]_i$) Response to Fluid Flow

MLO-Y4 cells were cultured in complete α-MEM+ on collagen coated slides at a density of 15×10^3 and 25×10^3 cells per slide. Following a 24 h incubation, the cells were treated with vehicle ± 50 or 500 μg/L of Co^{2+} and Cr^{3+} (1:1) for 30 min or 24 h, respectively. Following the treatments, cells were loaded with a 5 μM of Fluo-4AM (ThermoFisher Scientific), a fluorescent Ca^{2+} indicator for 45 min at 37°C to observe the cellular response to FSS. The cells were then subjected to 20 s of mechanical stimuli using a laminar fluid-flow chamber to create a physiologically relevant FSS of 16 dynes/cm^2, previously demonstrated to induce increases in $[Ca^{2+}]_i$ in vitro.[30–32] Changes in $[Ca^{2+}]_i$ were monitored in real-time using Leica AF6000 time-lapse fluorescent microscope. Cellular fluorescence of individual cells was measured using ImageJ (http://imagej.nih.gov/ij/) and the average change in fluorescence for each cell relative to baseline was calculated and plotted. The area under the curve (AUC), a measure of cellular response, and peak intensity were calculated using GraphPad Prism® (GraphPad Software, La Jolla, CA) and expressed relative to control from the same experimental time-point. All experiments were repeated three times with 40 cells analyzed for each experiment.

RT-PCR

Immediately following mechanical stimuli, RNA was extracted from MLO-Y4 cells using ReliaPrep™ RNA Cell Miniprep System (Promega, Southampton, UK) and reverse transcribed to cDNA using the High Capacity RNA-to-cDNA Kit (ThermoFisher Scientific). Quantitative RT-PCR was performed with 7900HT Fast Real-time PCR system using TaqMan® Gene expression assays (ThermoFisher Scientific) for *RANKL*, *Gp38*, *Dkk-1*, and *Cx43* and gene expression was expressed relative to *Gapdh* and controls with no exposure to metal ions and FSS using the ΔΔCT method. The expression of *Gapdh* did not vary across samples with respect to FSS and metal ion treatments (data not shown).

Mineralization Assay

MLO-A5 cells were seeded in 48-well plates at a density of 2×10^4 cells per well in 0.5 ml complete α-MEM till they reached confluence (usually day 3). The media was then replaced with vehicle ± metal ion treatments supplemented with 10 nM dexamethasone and 50 μg/ml L-ascorbic acid (Sigma–Aldrich) (referred to as osteogenic media) to promote osteoblast differentiation.[20,22,33] Vehicle ± metal ion treatments in osteogenic media was replenished every 2–3 days until 2 days prior to the end of experiment, when 5 mM inorganic phosphate was added to the osteogenic media to promote mineralization. On day 7 the cells were fixed overnight in 100% ethanol and stained with 40 mM Alizarin Red S (pH 4.2, Sigma–Aldrich). The plates were washed extensively with 95% ethanol and air-dried prior to scanning on a flatbed scanner. The percentage area of mineralization per well was quantified using ImageJ (http://imagej.nih.gov/ij/) and expressed as percentage response to vehicle.

Statistical Analysis

All experiments were conducted on three separate occasions with three minimum repeats per occasion. The average of the individual repeat experiments were then used for

statistical analysis. All values are reported as the mean ± standard deviation (SD) or mean ± 95% confidence interval (CI) and were analyzed using GraphPad Prism® (GraphPad Software). Data were tested for normality using the D'Agostino and Pearson omnibus normality test and analyzed by one-way analysis of variance (ANOVA) with post-test for linear trend or *t*-test to address specific questions. If a significant effect was found, specific interactions were examined by performing two-way analysis of variance with Sidak's multiple comparisons test. All tests were performed two-tailed using a critical *p*-value of 0.05.

RESULTS

Metal Ions Reduce MLO-Y4 Osteocyte Cell Number In Vitro

Co^{2+} ion treatment significantly decreased the number of MLO-Y4 cells over the full concentration range, while Cr^{3+} treatment had no effect on cell number (Fig. 1A). Combined metal ion treatment showed a significant interaction ($p = 0.0396$), reducing cell viability over the full concentration range (Fig. 1A and B), with 500 μg/L Co^{2+}:Cr^{3+} combined treatment having a greater effect over Co^{2+} treatment alone.

Metal Ions Increase the Dendricity of MLO-Y4 Cells In Vitro

Co^{2+} ion treatment increased the number of dendrites per cell over the full concentration range (Fig. 2A), while Cr^{3+} treatment had no significant effect. Combined metal ion treatment showed a significant interaction ($p = 0.0427$), with concentrations of 5,000 μg/L Co^{2+}:Cr^{+3} reducing the increase in dendrite number observed with Co^{2+} treatment alone. An increase in average length of MLO-Y4 dendrites was also observed with metal ion treatments. Co^{2+} treatment increased the number of dendrites over the full concentration range (Fig. 2B), while Cr^{3+} treatment had no significant effect. Co^{2+}:Cr^{3+} combined treatment similarly showed an increase in the number of dendrites over the full the concentration range (Fig. 2B) but no significant interaction was observed ($p = 0.6861$). The

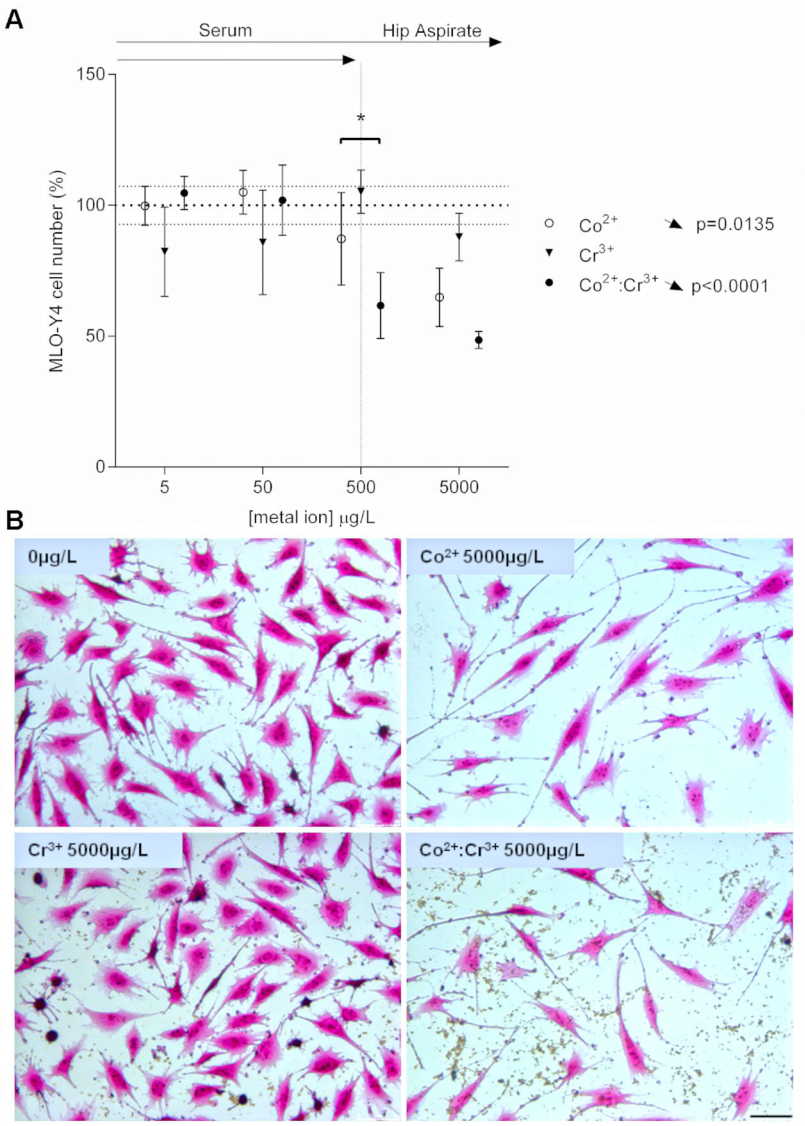

Figure 1. Effect of metal ions on MLO-Y4 cell number. (A) Graph depicts the changes in MLO-Y4 cell numbers following 24 h treatment with clinically relevant concentrations of Co^{2+}, Cr^{3+}, or Co^{2+}:Cr^{3+}. Cell numbers were counted from five non-overlapping random fields of view per well with four wells quantified for each treatment. All data are expressed as mean ± SD, relative to vehicle. Vertical dotted line separates the upper limit of previously reported ion concentrations equivalent to those in the patient serum and the hip aspirate. Significant linear trends across the concentration range analyzed using One-way ANOVA are represented by arrows in the corresponding direction of effect and *p*-values alongside the respective treatment condition. Asterisks are used to denote differences between Co^{2+} and combined Co^{2+}:Cr^{3+} treatments ($^*p < 0.05$). (B) MLO-Y4 cells stained with crystal violet—typical fields of view for vehicle (0 μg/L), Co^{2+} (5,000 μg/L), Cr^{3+} (5,000 μg/L), and Co^{2+}:Cr^{3+} (5,000 μg/L each), scale bar = 50 μm.

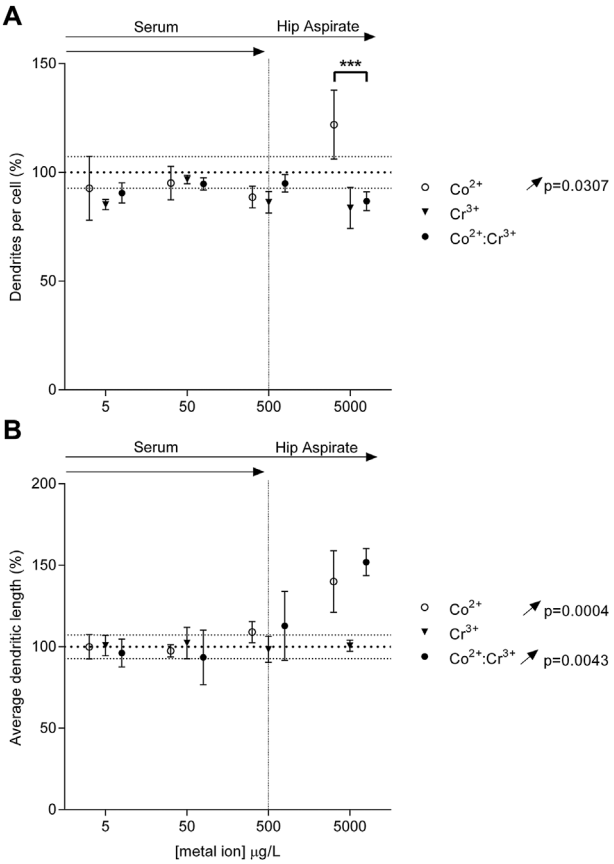

Figure 2. Metal ions increase the dendricity of MLO-Y4 cells in vitro. Graphs depict the changes in (A) dendrite number and (B) dendrite length per cell following 24 h treatment with clinically relevant concentrations of Co^{2+}, Cr^{3+}, or Co^{2+}:Cr^{3+}. Dendrite (>5 μm) numbers were counted and lengths measured for cells in five non-overlapping random fields of view per well with four wells quantified for each treatment. All data are expressed as mean ± SD, relative to vehicle. Vertical dotted line separates the upper limit of previously reported ion concentrations equivalent to those in the patient serum and the hip aspirate. Significant linear trends across the concentration range analyzed using One-way ANOVA are represented by arrows in the corresponding direction of effect and *p*-values alongside the respective treatment condition. Asterisks are used to denote differences between Co^{2+} and combined Co^{2+}:Cr^{3+} treatments ($^{***}p < 0.0001$).

combined Co^{2+}:Cr^{3+} treatment did not have any further effect over that of Co^{2+} alone.

Metal Ions Reduce the Intracellular Ca^{2+} Response in MLO-Y4 Following Mechanical Stimuli

The response of MLO-Y4 osteocyte cells to mechanical stimuli in the form of FSS was assessed by measuring intracellular Ca^{2+} changes in real time. Following 30 min and 24 h exposure to Co^{2+}:Cr^{3+}, a reduction in cellular response (AUC) to mechanical stimuli was observed for 50 and 500 μg/L compared to the vehicle (Fig. 3A and B). A reduction in the peak response was also observed for both 50 and 500 μg/L Co^{2+}:Cr^{3+}compared to the vehicle, for both time-points. The effects were dose-dependent with 500 μg/L Co^{2+}:Cr^{3+} showing reduced cellular and peak responses compared to 50 μg/L following 30 min and 24 h exposures.

MLO-Y4 Gene Expression in Response to FSS Is Altered With Metal Ion Exposure

The MLO-Y4 cells robustly expressed the osteocyte markers *Cx43* and *Gp38*, and the signaling molecules *RANKL* and *Dkk-1*, with the rank order of gene expression $Gp38 \geq Cx43 > RANKL > Dkk\text{-}1$ (data not shown). FSS resulted in increased expression of *RANKL* ($p = 0.0272$), *Gp38* ($p = 0.0017$), and *Cx43* ($p = 0.01148$), and a reduction in *Dkk-1* expression ($p = 0.0245$) compared to unstimulated cells (Fig. 4A). These changes in gene expression following FSS were also observed for the 24 h experimental group-increased *RANKL* ($p = 0.0415$), *Gp38* ($p = 0.0128$), and *Cx43* ($p = 0.0218$), and reduced *Dkk-1* ($p = 0.0245$) (Fig. 4B). Cells exposed to Co^{2+}:Cr^{3+} for 30 min and 24 h prior to FSS had blunted responses, with the osteocyte markers *Gp38* and *Cx43* showing reduced expression in significant linear trend over the concentration range (Fig. 4B, $p = 0.0338$ and $p = 0.0107$, respectively).

Metal Ions Reduce Mineralization by Late Osteoblast/Early Osteocyte MLO-A5 Cells

Using MLO-A5 cells, we found no effect of individual Co^{2+} ion treatment on mineralization. However, Cr^{3+} reduced the mineralization of the MLO-A5 cells over the concentration range equivalent to those observed in serum of patients with accelerated MOM bearing wear (Fig. 5), without affecting cell viability (data not shown). Combined metal ion treatment similarly showed a significant reduction in mineralization over the same concentration range; however, no interaction was seen ($p = 0.8257$) or any further effect of Co^{2+}:Cr^{+3} combined treatment over the effect of Cr^{3+} treatment alone.

DISCUSSION

The osteocyte is the most abundant type of bone cell and plays a critical role in mechanosensing and in the orchestration of bone remodeling. However, little is known about the effects of clinically relevant metal exposure on this bone cell population. Here, we show that exposure to increased Co^{2+} and Cr^{3+} concentrations is detrimental to osteocyte physiology. We find that osteocyte cell survival and dendritic morphology are sensitive to metal ions at concentrations seen clinically in patients with prostheses. We also show for the first time that the typical osteocytic response to FSS, including intracellular calcium signaling and gene expression of osteocyte markers and bone remodeling cytokines, is impaired in the presence of these metal ions.

Reduction in MLO-Y4 osteocyte cell viability after 24 h exposure to Co^{2+} occurred in a dose-dependent manner, consistent with and expanding on previous reports demonstrating a cytotoxic effect at high concentrations of Co^{2+} (0.05 mM; ~3,000 μg/L) following 48 h exposure.[25] The lack of any effect of Cr^{3+} alone is consistent with the observations of Kanaji and coworkers and the previously held dogma of the relative

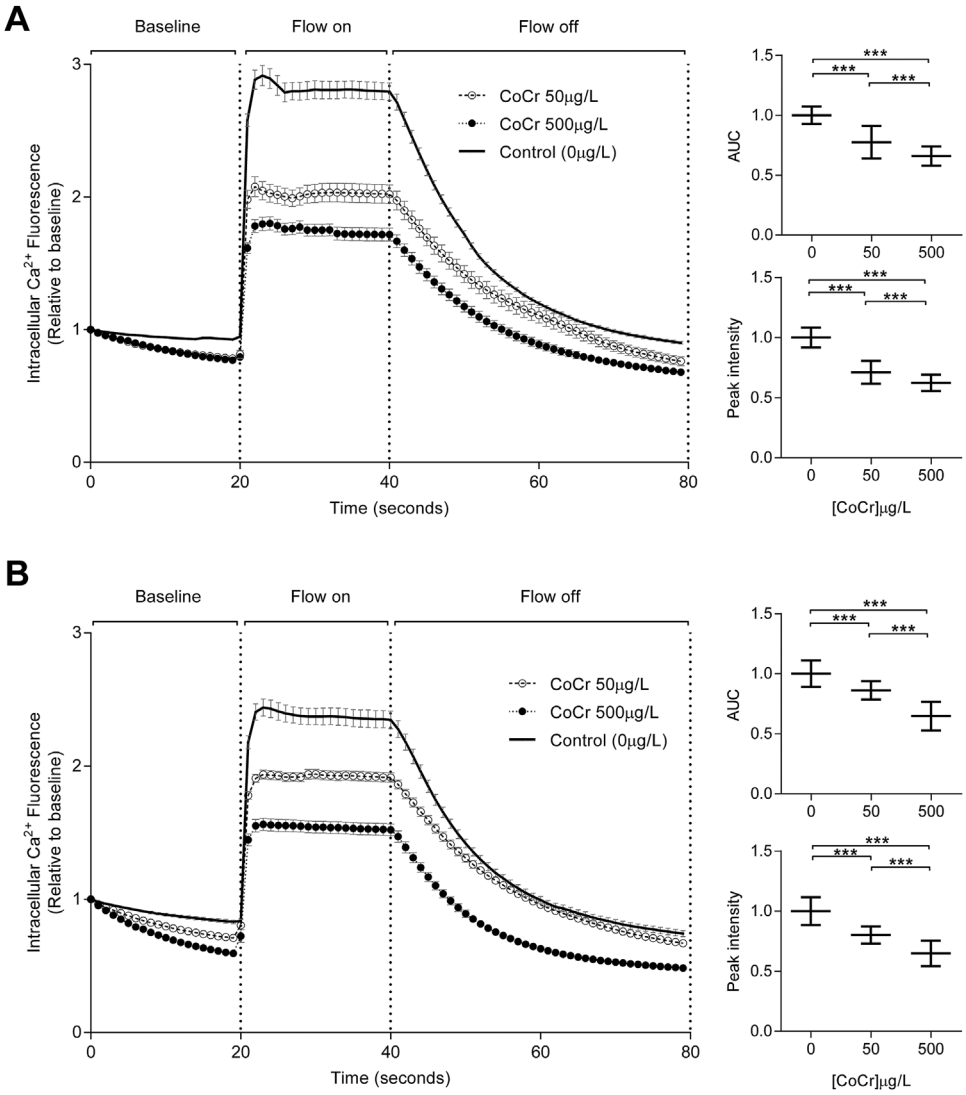

Figure 3. Metal ions reduce the intracellular Ca^{2+} response in MLO-Y4 following mechanical stimuli. The graphs illustrate changes in intracellular Ca^{2+} mediated fluorescence due to FSS (16 dynes/cm^2) following exposure to 50 and 500 μg/L of Co^{2+} and Cr^{3+} for (A) 30 min and (B) 24 h. Data are from three separate experiments with 40 cells analyzed for each experiment and are represented as mean ± 95%CI. The inset graphs illustrate the changes in area under curve (AUC) and peak intensity at both time points ($^{***}p < 0.0001$).

inability of Cr^{3+} to cross cell-membranes.[34] In contrast to this dogma, we have previously shown the intracellular localization of Cr^{3+} in osteoblasts,[21] as well as an additive effect of Co^{2+} and Cr^{3+} treatment.[22] Thus the increased effect of combined ions at 500 μg/L over the effect of Co^{2+} alone observed in this study suggests for the first time potential facilitation of Cr^{3+} entry into osteocytes, as well as common downstream signaling. The fact that we don't observe any increased effect with combined metal ion treatment for concentrations at the higher end equivalent to those observed in the patient hip aspirates suggests that Co^{2+} is having the dominate effect.

As osteoblasts transition to osteocytes and mature, they form dendritic processes and establish highly oriented intercellular communication between the vascular space and the bone surface.[1] Reduced osteocyte dendricity has a negative impact on osteocyte function and on the mechanical properties of bone.[35] Several diseased states have been associated with alterations in osteocyte dendricity. A decrease in interconnectivity has been observed in osteoporotic and osteoarthritic bone, while osteomalacic bone exhibits an increased interconnectivity which is chaotic.[4,5] We detected an increase in the number and length of dendrites in MLO-Y4 osteocytes cells treated with increasing concentrations of metal ions. One possible explanation for this observation is that it represents an attempt by the residual cell population to maintain or re-establish inter-cellular communication.

Osteocyte cell death plays a key role in the recruitment of osteoclasts and in bone resorption,[36] while dendrites are found increased in and orientated to regions of potential bone remodeling.[35] The reduction in osteocyte survival and increase in dendricity that we have observed in vitro at clinically relevant concen-

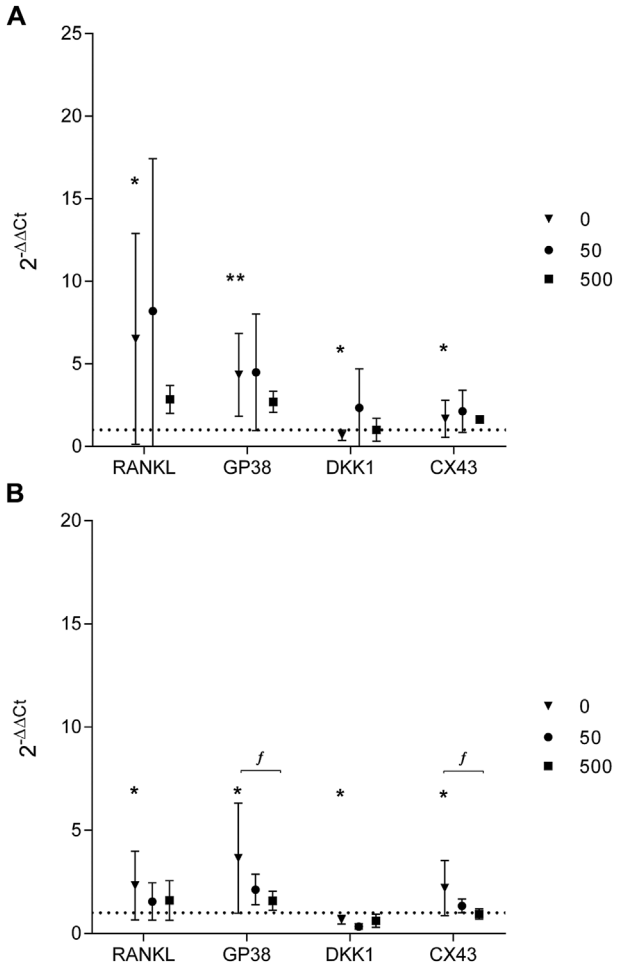

Figure 4. MLO-Y4 gene expression in response to fluid shear-stress is altered with metal ion exposure. The effect of FSS on osteocyte gene expression was assessed in the absence or presence of 50 and 500 μg/L of Co^{2+} and Cr^{3+} exposure for (A) 30 min and (B) 24 h. Changes in MLO-Y4 gene expression are depicted as $2^{-\Delta\Delta Ct}$ relative to *Gapdh* and untreated cells without application of FSS. All data are mean ± 95%CI from three separate experiments with three technical repeats per experiment. Comparisons between untreated cells and cells following FSS are represented by asterisks ($^{*}p < 0.05$; $^{**}p < 0.01$). Significant linear trends across the concentration range analyzed using one-way ANOVA with $p < 0.05$.are denoted as "*f*."

trations of metal ions may alter periprosthetic bone remodeling and may compound the previously reported direct effects observed on osteoblasts and osteoclasts.[20]

A change in intracellular calcium concentration is the immediate cellular response to mechanical stimuli and influences various downstream signaling events.[37] Consistent with this, fluid flow-induced increases in calcium signaling in MLO-Y4 cells were significantly reduced by combined metal ion treatment in a dose dependent manner, thus confirming a detrimental effect on osteocyte function. Furthermore, the mechano-responsive genes that are known to be upregulated in response to mechanical loading are increased in our system with fluid flow.[35,38–41] Exposure to metal ions suppressed the increased expression of osteocyte markers *Gp38* and *Cx43* after 24 h, but had no effect on the fluid flow-induced effects on *RANKL* or DKK1 expression. While *Gp38* is an early response gene responsible for dendrite elongation,[35] *Cx43* is involved cell–cell communication by forming gap-junctions and "hemi-channels."[42] It has been shown that prostaglandin E2 (PGE2) signaling from osteocytes occurs via *Cx43* following mechanical strain[42] and mediates its osteogenic effect. The lack of upregulation of *Cx43* with FSS following metal exposure may impede this autocrine/paracrine regulation of periprosthetic adaptive bone remodeling in patients with elevated metal levels. We appreciate that the selection of candidate genes in this study does not provide a comprehensive overview of the effects osteocytes might have on periprosthetic bone remodeling, but it does suggest an aberrance in regulation following FSS.

Finally, using the late osteoblasts/early osteocytes cell line MLO-A5 we found that Co^{2+} exposure had no effect on mineralization, but Cr^{3+} treatment inhibited mineralization in a dose dependent manner, while the MLO-A5 cells remained viable and produced a matrix that was left unmineralized. It is known that mineralization by osteoid-osteocyte cells occurs via the release of mineralized spheres that nucleate collagen fibrils and propagate calcification,[43] and there is evidence that Cr^{3+} can form complexes with amino acids in collagen distorting its helical backbone.[44] Therefore, Cr^{3+}-related distortion of the collagen structure may perturb matrix nucleation and eventual mineralization by MLO-A5 cells, as seen in this study.

We acknowledge that our study has limitation due to use of the osteocyte-like cell lines. Although recent studies have described methods for extraction of primary osteocytes from mouse long bones,[45] the yields are generally low and would not have been sufficient for our experimental purposes. Therefore, we have used the MLO-Y4 cell line which serve as a good osteocyte model as they respond to mechanical stimulation by releasing prostaglandin-E_2,[46] ATP,[47] and nitric oxide,[48] integral to osteocytes' orchestration of adaptive bone remodeling. We also used MLO-A5 cells with their higher expression of ALP and osteocalcin represent cells undergoing osteoblast–osteocyte transition which have the ability to mineralize the osteoid matrix they are embedded in.[27] Used together, we believe that these models are a good representation of osteocyte behavior with which to test our hypothesis, although we appreciate that some of the key regulators of bone homeostasis such as SOST/sclerostin and FGF23 are not expressed by these cell lines.[49,50]

In conclusion, our current data suggest that metal ions directly affect osteocyte cell number and dendricity. In addition, we have shown that the functional responses and gene expression following FSS is blunted in osteocytes exposed to metal ions with implications for adaptive bone remodeling in patients with prosthesis tribocorrosion.

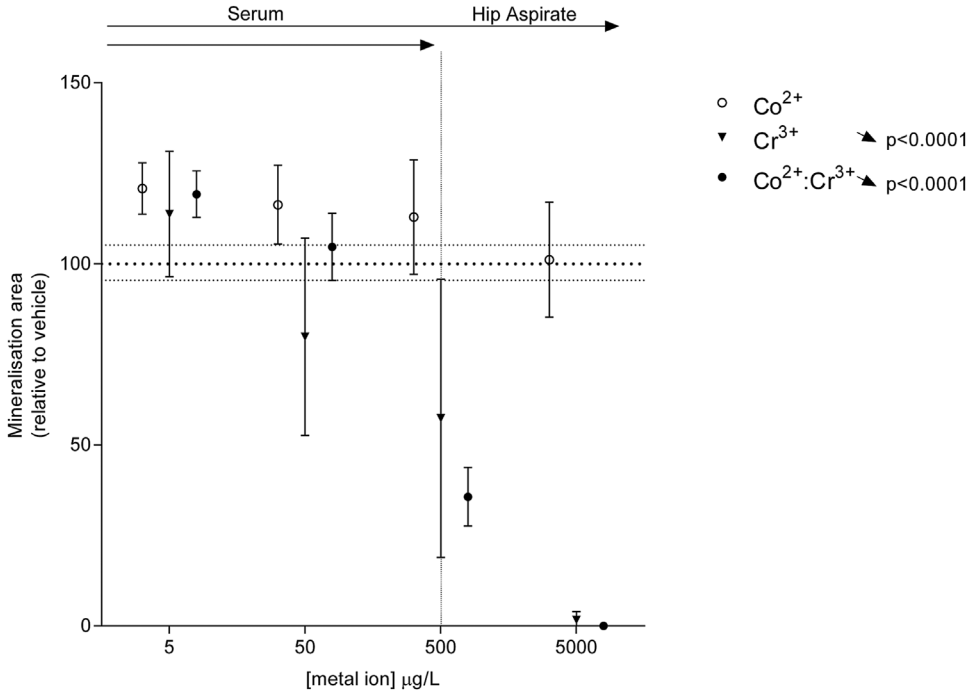

Figure 5. Metal ions reduce mineralization by late osteoblast/early osteocyte MLO-A5 cells. Percentage area mineralized by MLO-A5 cells following exposure to clinically relevant concentrations of Co^{2+} and Cr^{3+}. All data are expressed as mean ± SD, relative to vehicle. Vertical dotted line separates the upper limit of previously reported ion concentrations equivalent to those in the patient serum and the hip aspirate. Significant linear trends across the concentration range analyzed using one-way ANOVA are represented by arrows in the corresponding direction of effect and *p*-values alongside the respective treatment condition.

AUTHORS' CONTRIBUTIONS

KMS and PO: substantial contributions to research design, or the acquisition, analysis, or interpretation of data and drafting the paper or revising it critically. NM: substantial contributions to research design, or the acquisition, analysis, or interpretation of data. JMW and AG: substantial contributions to research design, or the acquisition, analysis, or interpretation of data; drafting the paper or revising it critically; and approval of the submitted version.

ACKNOWLEDGMENTS

The authors would like to thank ORUK for funding to KMS (Project 517), Arthritis Research UK for funding to both PO and NM, The University of Sheffield LETS SURE scheme for funding to PO and Dr. Mo Sacoor MRCP Medical Elective Research Scholarship for funding PO.

REFERENCES

1. Bonewald LF. 2011. The amazing osteocyte. J Bone Miner Res 26:229–238.
2. Klein-Nulend J, Bakker AD, Bacabac RG, et al. 2013. Mechanosensation and transduction in osteocytes. Bone 54:182–190.
3. Weinstein RS. 2012. Glucocorticoid-induced osteonecrosis. Endocrine 41:183–190.
4. Jaiprakash A, Prasadam I, Feng JQ, et al. 2012. Phenotypic characterization of osteoarthritic osteocytes from the sclerotic zones: a possible pathological role in subchondral bone sclerosis. Int J Biol Sci 8:406–417.
5. Knothe Tate ML, Adamson JR, Tami AE, et al. 2004. The osteocyte. Int J Biochem Cell Biol 36:1–8.
6. de Steiger RN, Hang JR, Miller LN, et al. 2011. Five-year results of the ASR XL acetabular system and the ASR Hip Resurfacing System: an analysis from the Australian Orthopaedic Association National Joint Replacement Registry. J Bone Joint Surg Am 93:2287–2293.
7. Graves SE, Rothwell A, Tucker K, et al. 2011. A multinational assessment of metal-on-metal bearings in hip replacement. J Bone Joint Surg Am 93:43–47.
8. Smith AJ, Dieppe P, Howard PW, et al. 2012. Failure rates of metal-on-metal hip resurfacings: analysis of data from the National Joint Registry for England and Wales. Lancet 380:1759–1766.
9. Smith AJ, Dieppe P, Vernon K, et al. 2012. Failure rates of stemmed metal-on-metal hip replacements: analysis of data from the National Joint Registry of England and Wales. Lancet 379:1199–1204.
10. Hannemann F, Hartmann A, Schmitt J, et al. 2013. European multidisciplinary consensus statement on the use and monitoring of metal-on-metal bearings for total hip replacement and hip resurfacing. Orthop Traumatol Surg Res 99:263–271.
11. US Food and Drug Administration. 2014. Recalls – Metal-on-metal Hip Implants. http://www.fda.gov/MedicalDevices/ProductsandMedicalProcedures/ImplantsandProsthetics/MetalonMetalHipImplants/ucm241770.htm
12. Gilbert JL, Buckley CA, Jacobs JJ. 1993. In vivo corrosion of modular hip prosthesis components in mixed and similar metal combinations. The effect of crevice, stress, motion, and alloy coupling. J Biomed Mater Res 27:1533–1544.
13. McKellop HA, Sarmiento A, Brien W, et al. 1992. Interface corrosion of a modular head total hip prosthesis. J Arthroplasty 7:291–294.
14. Plummer DR, Berger RA, Paprosky WG, et al. 2016. Diagnosis and management of adverse local tissue reactions second-

ary to corrosion at the head-neck junction in patients with metal on polyethylene bearings. J Arthroplasty 31:264–268.
15. Cieslak W, Pap K, Bunch DR, et al. 2013. Highly sensitive measurement of whole blood chromium by inductively coupled plasma mass spectrometry. Clin Biochem 46:266–270.
16. Tvermoes BE, Finley BL, Unice KM, et al. 2013. Cobalt whole blood concentrations in healthy adult male volunteers following two-weeks of ingesting a cobalt supplement. Food Chem Toxicol 53:432–439.
17. Grubl A, Marker M, Brodner W, et al. 2007. Long-term follow-up of metal-on-metal total hip replacement. J Orthop Res 25:841–848.
18. Lass R, Grubl A, Kolb A, et al. 2014. Comparison of synovial fluid, urine, and serum ion levels in metal-on-metal total hip arthroplasty at a minimum follow-up of 18 years. J Orthop Res 32:1234–1240.
19. Davda K, Lali FV, Sampson B, et al. 2011. An analysis of metal ion levels in the joint fluid of symptomatic patients with metal-on-metal hip replacements. J Bone Joint Surg Br 93:738–745.
20. Andrews RE, Shah KM, Wilkinson JM, et al. 2011. Effects of cobalt and chromium ions at clinically equivalent concentrations after metal-on-metal hip replacement on human osteoblasts and osteoclasts: implications for skeletal health. Bone 49:717–723.
21. Shah KM, Quinn PD, Gartland A, et al. 2015. Understanding the tissue effects of tribo-corrosion: uptake, distribution, and speciation of cobalt and chromium in human bone cells. J Orthop Res 33:114–121.
22. Shah KM, Wilkinson JM, Gartland A. 2015. Cobalt and chromium exposure affects osteoblast function and impairs the mineralization of prosthesis surfaces in vitro. J Orthop Res 33:1663–1670.
23. Hinoi E, Ochi H, Takarada T, et al. 2012. Positive regulation of osteoclastic differentiation by growth differentiation factor 15 upregulated in osteocytic cells under hypoxia. J Bone Miner Res 27:938–949.
24. Kanaji A, Caicedo MS, Virdi AS, et al. 2009. Co-Cr-Mo alloy particles induce tumor necrosis factor alpha production in MLO-Y4 osteocytes: a role for osteocytes in particle-induced inflammation. Bone 45:528–533.
25. Kanaji A, Orhue V, Caicedo MS, et al. 2014. Cytotoxic effects of cobalt and nickel ions on osteocytes in vitro. J Orthop Surg Res 9:91.
26. Orhue V, Kanaji A, Caicedo MS, et al. 2011. Calcineurin/nuclear factor of activated T cells (NFAT) signaling in cobalt-chromium-molybdenum (CoCrMo) particles-induced tumor necrosis factor-alpha (TNFalpha) secretion in MLO-Y4 osteocytes. J Orthop Res 29:1867–1873.
27. Kato Y, Boskey A, Spevak L, et al. 2001. Establishment of an osteoid preosteocyte-like cell MLO-A5 that spontaneously mineralizes in culture. J Bone Miner Res 16:1622–1633.
28. Kato Y, Windle JJ, Koop BA, et al. 1997. Establishment of an osteocyte-like cell line, MLO-Y4. J Bone Miner Res 12:2014–2023.
29. Rosser J, Bonewald LF. 2012. Studying osteocyte function using the cell lines MLO-Y4 and MLO-A5. Methods Mol Biol 816:67–81.
30. Price C, Zhou X, Li W, et al. 2011. Real-time measurement of solute transport within the lacunar-canalicular system of mechanically loaded bone: direct evidence for load-induced fluid flow. J Bone Miner Res 26:277–285.
31. Rath AL, Bonewald LF, Ling J, et al. 2010. Correlation of cell strain in single osteocytes with intracellular calcium, but not intracellular nitric oxide, in response to fluid flow. J Biomech 43:1560–1564.
32. Weinbaum S, Cowin SC, Zeng Y. 1994. A model for the excitation of osteocytes by mechanical loading-induced bone fluid shear stresses. J Biomech 27:339–360.
33. Gartland A, Rumney RMH, Dillon JP, et al. 2012. Isolation and culture of human osteoblasts. In: Mitry RR, Hughes DR, editors. Human cell culture protocols. Totowa, NJ: Humana Press. p 337–355.
34. Gray SJ, Sterling K. 1950. The tagging of red blood cells and plasma proteins with radioactive chromium. J Clin Invest 29:818.
35. Zhang K, Barragan-Adjemian C, Ye L, et al. 2006. E11/gp38 selective expression in osteocytes: regulation by mechanical strain and role in dendrite elongation. Mol Cell Biol 26:4539–4552.
36. Verborgt O, Tatton NA, Majeska RJ, et al. 2002. Spatial distribution of Bax and Bcl-2 in osteocytes after bone fatigue: complementary roles in bone remodeling regulation? J Bone Miner Res 17:907–914.
37. Lu XL, Huo B, Park M, et al. 2012. Calcium response in osteocytic networks under steady and oscillatory fluid flow. Bone 51:466–473.
38. Alford AI, Jacobs CR, Donahue HJ. 2003. Oscillating fluid flow regulates gap junction communication in osteocytic MLO-Y4 cells by an ERK1/2 MAP kinase-dependent mechanism. Bone 33:64–70.
39. Cheng B, Zhao S, Luo J, et al. 2001. Expression of functional gap junctions and regulation by fluid flow in osteocyte-like MLO-Y4 cells. J Bone Miner Res 16:249–259.
40. You L, Temiyasathit S, Lee P, et al. 2008. Osteocytes as mechanosensors in the inhibition of bone resorption due to mechanical loading. Bone 42:172–179.
41. Kulkarni RN, Bakker AD, Everts V, et al. 2010. Inhibition of osteoclastogenesis by mechanically loaded osteocytes: involvement of MEPE. Calcif Tissue Int 87:461–468.
42. Cherian PP, Siller-Jackson AJ, Gu S, et al. 2005. Mechanical strain opens connexin 43 hemichannels in osteocytes: a novel mechanism for the release of prostaglandin. Mol Biol Cell 16:3100–3106.
43. Barragan-Adjemian C, Nicolella D, Dusevich V, et al. 2006. Mechanism by which MLO-A5 late osteoblasts/early osteocytes mineralize in culture: similarities with mineralization of lamellar bone. Calcif Tissue Int 79:340–353.
44. Wu B, Mu C, Zhang G, et al. 2009. Effects of Cr3+ on the structure of collagen fiber. Langmuir 25:11905–11910.
45. Stern AR, Stern MM, Van Dyke ME, et al. 2012. Isolation and culture of primary osteocytes from the long bones of skeletally mature and aged mice. Biotechniques 52:361–373.
46. Kamel MA, Picconi JL, Lara-Castillo N, et al. 2010. Activation of beta-catenin signaling in MLO-Y4 osteocytic cells versus 2T3 osteoblastic cells by fluid flow shear stress and PGE2: implications for the study of mechanosensation in bone. Bone 47:872–881.
47. Kringelbach TM, Aslan D, Novak I, et al. 2015. Fine-tuned ATP signals are acute mediators in osteocyte mechanotransduction. Cell Signal 27:2401–2409.
48. Vatsa A, Mizuno D, Smit TH, et al. 2006. Bio imaging of intracellular NO production in single bone cells after mechanical stimulation. J Bone Miner Res 21:1722–1728.
49. Woo SM, Rosser J, Dusevich V, et al. 2011. Cell line IDG-SW3 replicates osteoblast-to-late-osteocyte differentiation in vitro and accelerates bone formation in vivo. J Bone Miner Res 26:2634–2646.
50. Yang W, Harris MA, Heinrich JG, et al. 2009. Gene expression signatures of a fibroblastoid preosteoblast and cuboidal osteoblast cell model compared to the MLO-Y4 osteocyte cell model. Bone 44:32–45.